The sea ice momentum equation in the free drift regime

Elizabeth C. Hunke and John K. Dukowicz
T-3 Fluid Dynamics Group, Los Alamos National Laboratory
Tech. Rep. LA-UR-03-2219

April 8, 2003

Abstract

The form of the momentum equation used in large-scale climate models to describe sea ice drift has come under question, especially regarding the ice behavior in regions where ice concentration is low. In this short note, we seek to illuminate the source of the controversy and give a careful explanation of how the matter is addressed in our model. We begin with an overview of the model derivation to place the issue in context, narrow the discussion to the free drift regime, then present results from a simulation comparison that indicate the relative importance of changes made in the model.

1 Fundamentals

The vertically integrated, two-dimensional momentum equation generally applied in large-scale sea ice models [5, for example] is

$$\rho h \frac{\partial \mathbf{u}}{\partial t} = \nabla_2 \cdot \sigma + F(\mathbf{u}), \tag{1}$$

where $\mathbf{u}$ is the horizontal velocity vector (m/s), ρ represents (constant) ice density (kg/m^3), h is the actual thickness of the ice, $\nabla_2 \cdot \sigma$ is the horizontal divergence of the internal ice stress tensor, and F represents surface (atmosphere and ocean drag) and body (Coriolis, sea surface tilting) forces acting on the ice (N/m^2),

$$F(\mathbf{u}) = \tau_a + \tau_w(\mathbf{u}) + \tau_{cor}(\mathbf{u}) + \tau_{tilt}. \tag{2}$$

Here we have indicated the standard velocity dependence of the forcing terms. Eq. (1) may be derived from the equations of continuum mechanics [1], in which the local velocity, $\tilde{\mathbf{u}}$, is determined from

$$\rho \frac{\partial \tilde{\mathbf{u}}}{\partial t} = \nabla_3 \cdot \tilde{\sigma} + F_b, \tag{3}$$

Here, $\tilde{\sigma}$ is the local stress tensor (N/m^2) and F_b represents body forcing terms acting on the ice associated with gravity (sea surface tilting) and the Coriolis effect.

We are interested only in the horizontal components of the ice motion. Integrate Eq. (3) over the volume of ice in a grid cell of area A,

$$\int_A \int_0^h \rho \frac{\partial \tilde{\mathbf{u}}}{\partial t}\, dz\, dA = \int_A \int_0^h \left(\nabla_3 \cdot \tilde{\sigma} + F_b\right)\, dz\, dA. \tag{4}$$

Assuming that the volume of integration is an arbitrary "pillbox" with vertical surfaces on the sides, we apply the divergence theorem to the first term on the right hand side of (4):

$$\begin{aligned}
\int_A \int_0^h \nabla_3 \cdot \tilde{\sigma}\, dz\, dA &= \oint_{\partial V} \hat{\mathbf{n}} \cdot \tilde{\sigma}\, dS_2 \\
&= \oint_{\partial A} \hat{\mathbf{n}} \cdot \tilde{\sigma}\, (h\, dS_1) + \tilde{\sigma}_z(h) - \tilde{\sigma}_z(0) \\
&= \int_A \nabla \cdot (h\tilde{\sigma})\, dA + \tilde{\sigma}_z(h) - \tilde{\sigma}_z(0).
\end{aligned}$$

The $\tilde{\sigma}_z$ terms represent forcing on the ice surface by the atmosphere and ocean, generally modeled as

$$\begin{aligned} \tau_a &\propto |\mathbf{U}_a|\,\mathbf{U}_a, \\ \tau_w &\propto |\mathbf{U}_w - \mathbf{u}|\,(\mathbf{U}_w - \mathbf{u}), \end{aligned}$$

where $\mathbf{U}_a$ and $\mathbf{U}_w$ are wind and ocean current velocities, respectively [5]. We define $\sigma = h\tilde{\sigma}$, noting that h is included in the definitions of the bulk and shear viscosities and the ice strength P used to define σ in [5]. Additionally assuming that the velocity and the body force are vertically uniform, Eq. (4) may be written

$$\int_A \rho h \frac{\partial \mathbf{u}}{\partial t}\, dA = \int_A \nabla_2 \cdot \sigma\, dA + \int_A (\tau_a + \tau_w + hF_b)\, dA.$$

Since the horizontal area of integration is arbitrary, this implies Eq. (1). In the numerical model we average the momentum equation over the grid cell area; *i.e.*, we solve

$$\frac{1}{A}\int_A \rho h \frac{\partial \mathbf{u}}{\partial t}\, dA = \frac{1}{A}\int_A \nabla_2 \cdot \sigma\, dA + \frac{1}{A}\int_A (\tau_a + \tau_w + hF_b)\, dA. \tag{5}$$

2 Free drift in the marginal ice zone

2.1 Statement of the problem

The derivation above assumes that the ice is a continuum material, distributed uniformly over the grid cell. In cells without ice, the velocity in Eq. (5) is that of the interface between the atmosphere and the ocean, and in partially ice covered cells, the velocity represents an average of the ice velocity and that of the interface over open water. As discussed below, we have been making a crude numerical approximation in assuming that the computed velocity is that of the ice itself. This complicates comparison of model results with observations, particularly in the marginal ice zone where the ice is undergoing free drift.

In the model, the free drift approximation occurs when $\nabla_2 \cdot \sigma = 0$. This is obtained in low ice concentration regions by setting the ice strength to zero, $P = 0$, so that, assuming a quasi-steady state,

$$\frac{1}{A}\int_A F(\mathbf{u}) dA = 0. \tag{6}$$

This gives the computed velocity in areas of thin ice or low ice concentration (less than 85% in our current model), including areas with no ice at all. Because the Coriolis and tilting terms (hF_b in Eq. (5)) depend on the ice mass but the atmosphere and ocean drag terms do not, the velocity computed from (6) depends on the ice concentration. In particular, if the forcing and ice thickness are the same in two grid cells but the concentrations differ slightly, then the velocities in the grid cells will differ. This conflicts with pointwise free drift theory, which asserts that the *actual* (not cell-averaged) ice velocity should be uniform under uniform forcing, regardless of the concentration itself.

2.2 Resolution of the problem

In the integral equation (5), we may include what we know about the forces and $\mathbf{u}$ in the ice-free areas to obtain a better approximation for the actual ice velocity in a grid cell. Where $h = 0$, (5) reduces to

$$\frac{1}{A}\int_{(1-c)A} [\tau_a + \tau_w(\mathbf{u})]\, dA = 0,$$

and hence

$$\frac{1}{A}\int F(\mathbf{u}) dA = \frac{1}{A}\int_{cA} F(\mathbf{u}) dA,$$

where c is the ice covered area fraction. Therefore the only contribution of the forcing terms in Eq. (2) to the momentum equation is from the sum of those terms over the ice covered fraction of the grid cell;

over the ice-free fraction, their sum is zero. [**NB** The individual terms are not zero themselves, only the sum is zero.]

This change does *not* represent a change in our interpretation of the forcing terms in (5); they still represent an average over the entire grid cell, but now the computed average is more accurate due to partitioning of the grid cell into ice covered and ice-free areas. The internal ice stress term in (5) can not be reduced to ice-free and ice covered portions easily because of the continuum assumption made in deriving the model, although we do assume that it is zero in low ice concentration regions for purposes of computing free drift.

Although the velocity in the continuum equation necessarily represents an average over the entire grid cell, we make an approximation that is tantamount to assuming that the computed velocity, $\overline{\mathbf{u}}$, represents an average over just the ice-covered portion of the cell, or more simply, that all of the ice in the cell is moving at the same velocity:

$$\begin{aligned} \frac{1}{A}\int_A \rho h \frac{\partial \mathbf{u}}{\partial t}\, dA &= \frac{1}{A}\int_{cA} \rho h \frac{\partial \mathbf{u}}{\partial t}\, dA \\ &= \left(\frac{1}{A}\int_{cA} \rho h\, dA\right)\left(\frac{\int_{cA} \rho h \frac{\partial \mathbf{u}}{\partial t}\, dA}{\int_{cA} \rho h\, dA}\right) \\ &= m\left\langle \frac{\partial \mathbf{u}}{\partial t} \right\rangle \approx m\frac{\partial \overline{\mathbf{u}}}{\partial t}, \end{aligned} \tag{7}$$

where m is ice mass per unit (grid cell) area. The approximation enters because the time derivative of mass is nonzero.

2.3 Implementation

In our numerical model, the various terms in (2) are computed separately. We currently compute the surface wind stress over each thickness of ice, aggregate those into an average quantity over ice, and then scale the result to the entire grid cell area (because the surface stress over open water, τ_{a0}, is computed elsewhere, not in the ice component model of the fully coupled CCSM system). That is, the area averaged wind stress over a grid cell should be computed properly as

$$\frac{1}{A}\int \tau_a\, dA \sim \sum_{n=0}^{N} c_n \tau_{an} = c_0\tau_{a0} + \sum_{n=1}^{N} c_n \tau_{an},$$

where $n = 1, ..., N$ represent categories with finite ice thickness and c_0 is the ice-free area fraction, but because the ice model does not "know" τ_{a0}, we approximate the average wind stress over the full grid cell as

$$\frac{1}{A}\int \tau_a\, dA \sim \frac{1}{c}\sum_{n=1}^{N} c_n \tau_{an}.$$

However, because the sum of the forces over the ice-free area is zero, in fact we do not need to know τ_{a0}; it cancels with the equivalent ice-ocean stress in the ice-free area of the cell. Therefore we apply only the portion of the wind stress and ocean stress over the ice-covered area,

$$\sum_{n=1}^{N} (c_n \tau_{an}) + c\tau_w(\overline{\mathbf{u}}). \tag{8}$$

This simply involves removing the division of air stress by ice area fraction and multiplying the standard ocean stress term by the ice area fraction. For coupled runs, the wind and ocean stresses over/under the ice, given by (8), still need to be divided by c in order to be converted to the equivalent (unphysical) full grid cell quantity (actually stress per unit ice area), as per the CCSM coupling conventions.

The Coriolis and tilting terms already incorporate the ice concentration through the ice mass per unit area, thus requiring no change to the code. These terms are not sent to the coupler.

3 Simulation results

3.1 Model configuration

Comparison of results from two simulations, with and without the ice concentration correction to the wind and ocean terms (the test run and the control run, respectively), reveals the relative importance of this correction. We compare results after 30 model years from a coupled ice-ocean model. The simulations were run on a nominally 3° resolution global mesh (100x116 with 25 ocean depth levels) in which the north pole singularity has been moved smoothly into Greenland. The grid is shown in Fig. 1.

The Parallel Ocean Program (POP) [9, 3, 4] is a member of the Bryan-Cox family of z-coordinate ocean models, featuring hydrostatic, Boussinesq primitive equations for ocean temperature, salinity and momentum, and an implicit free surface. The ocean model provides sea surface temperature, salinity, currents, slope and a freezing or melting potential to the ice model. Additional information regarding the POP ocean model can be obtained from
http://www.acl.lanl.gov/climate/models/pop/documentation/popdoc_frames.htm; here we describe only the model aspects most pertinent for the comparison simulations.

The Los Alamos sea ice model, CICE, features energy conserving thermodynamics along with energy-based ridging and ice strength using an ice thickness distribution with five ice thickness categories, and an incremental remapping advection scheme. The momentum equation is part of the elastic-viscous-plastic dynamics component [5, 6]. The ice model provides a fresh water flux, net heat flux and ice-ocean stress to the ocean model. The ice model is fully documented in [7].

The ice and ocean models are coupled via a modified version of the "flux coupler" developed jointly at the National Center for Atmospheric Research (NCAR) and Los Alamos National Laboratory [2]. The coupler serves as a driver for and interface between the component models: CICE, POP, and a third component that reads atmospheric data from files and prepares the data for use by the other components. The coupler merges ice and ocean quantities based on the ice area fraction in cells where there is less than 100% ice coverage. Momentum exchange is accomplished through a quadratic ice-ocean drag term computed by the ice model using level 1 currents.

Wind velocity, specific humidity, air density and potential temperature are used to compute stability-dependent transfer coefficients used in formulas for the surface wind stress and turbulent heat fluxes over both ice and ocean. The 1979–1988 atmospheric forcing data includes six-hourly, T62 resolution, 10 m data for air temperature, air density, specific humidity, and wind velocity from the National Centers for Environmental Prediction (NCEP) reanalyses, International Satellite Cloud Climatology Project (ISCCP) [8] monthly downward shortwave radiation flux and cloud fraction, and monthly precipitation fields (MSU) [10]. The model also incorporates a monthly climatology for river runoff.

3.2 Results

Fig. 2 shows the difference in ice area and velocity for January of year 30. As expected, the largest differences occur in the marginal ice zone where the ice concentration is low. This area comprises the ice edge in the winter (northern) hemisphere and most of the pack in the summer (southern) hemisphere. Figs. 3 and 4 show the ice area and velocity for the control run and the corresponding difference plots for January and July in the Arctic. These plots are cut out from the top left corner of the logical grid shown in Fig. 2; Greenland lies along the top, Iceland is the large island to the left, Spitzbergen is the island near the upper center, and the Eurasian continent is the land mass at the bottom of these plots. Alaska is in the lower right corner.

Differences in the ice area are minor except near the ice edge, where the concentration is less that about 90%. The biggest difference for ice velocity appears to be direction. Reduced wind stress would make the ice drift slower, but reduced ocean drag compensates for that somewhat; the Coriolis term in the test run is more important relative to the wind and ocean stresses than in the control run, resulting in turning of the velocity vectors.

Fig. 5 indicates the effect of this change in the ice model on the simulated ocean characterics. Near the ice edge, the mean annual sea surface temperature (SST) reflects the change in ice area, with cooler temperatures where there is more ice coverage in the test run and warmer temperatures where there is

less ice. The velocity difference vectors reflect the relative turning of the ice motion in the test run with respect to the control, with generally slower surface currents. Note that there are changes in the SST and surface currents even in the North Atlantic, far from the sea ice edge. These changes are transmitted through the ocean, as the ice velocity is zero in grid cells where there is no ice.

Although the changes in the ice and ocean simulation are widespread, they are relatively small. We observe differences in the details of the simulation, but we do not expect these changes to significantly affect the simulated climate. However, the change to the model described above is important because it makes the simulation more accurate, in the sense that it now takes into account physical information about the ice-free areas that was merely estimated in the control run.

Acknowledgments

We gratefully acknowledge Jonathan Gregory and Alison McLaren of the U.K. Met Office, Hadley Centre, and William Connolley of the British Antarctic Survey for bringing this issue to our attention. This work was performed within the Department of Energy Climate Change Prediction Program.

References

[1] G. K. Batchelor. *An Introduction to Fluid Dynamics*. Cambridge University Press, 1967. 615 pp.

[2] F. O. Bryan, B. G. Kauffman, W. G. Large, and P. R. Gent. The NCAR CSM flux coupler. Technical Note TN-425+STR, National Center for Atmospheric Research, May 1996.

[3] J. K. Dukowicz, R. D. Smith, and R. C. Malone. A reformulation and implementation of the Bryan-Cox-Semtner ocean model on the connection machine. *J. Atmos. Oceanic Technol.*, 10:195–208, 1993.

[4] J. K. Dukowicz, R. D. Smith, and R. C. Malone. Implicit free-surface method for the Bryan-Cox-Semtner ocean model. *J. Geophys. Res.–Oceans*, 99:7991–8014, 1994.

[5] E. C. Hunke and J. K. Dukowicz. An elastic-viscous-plastic model for sea ice dynamics. *J. Phys. Oceanogr.*, 27:1849–1867, 1997.

[6] E. C. Hunke and J. K. Dukowicz. The Elastic-Viscous-Plastic sea ice dynamics model in general orthogonal curvilinear coordinates on a sphere—Effect of metric terms. *Mon. Wea. Rev.*, 2001. In review.

[7] E. C. Hunke and W. H. Lipscomb. CICE: the Los Alamos Sea Ice Model, Documentation and Software, version 3. Technical Report LA-CC-98-16, Los Alamos National Laboratory, Los Alamos, New Mexico, 2001.

[8] W. B. Rossow and R. A. Schiffer. ISCCP cloud data products. *Bull. Amer. Meteor. Soc.*, 72:2–20, 1991.

[9] R. D. Smith, J. K. Dukowicz, and R. C. Malone. Parallel ocean general circulation modeling. *Physica D*, 60:38–61, 1992.

[10] R. W. Spencer. Global oceanic precipitation from the MSU during 1979–91 and comparisons to other climatologies. *J. Clim.*, 6:1301–1326, 1993.

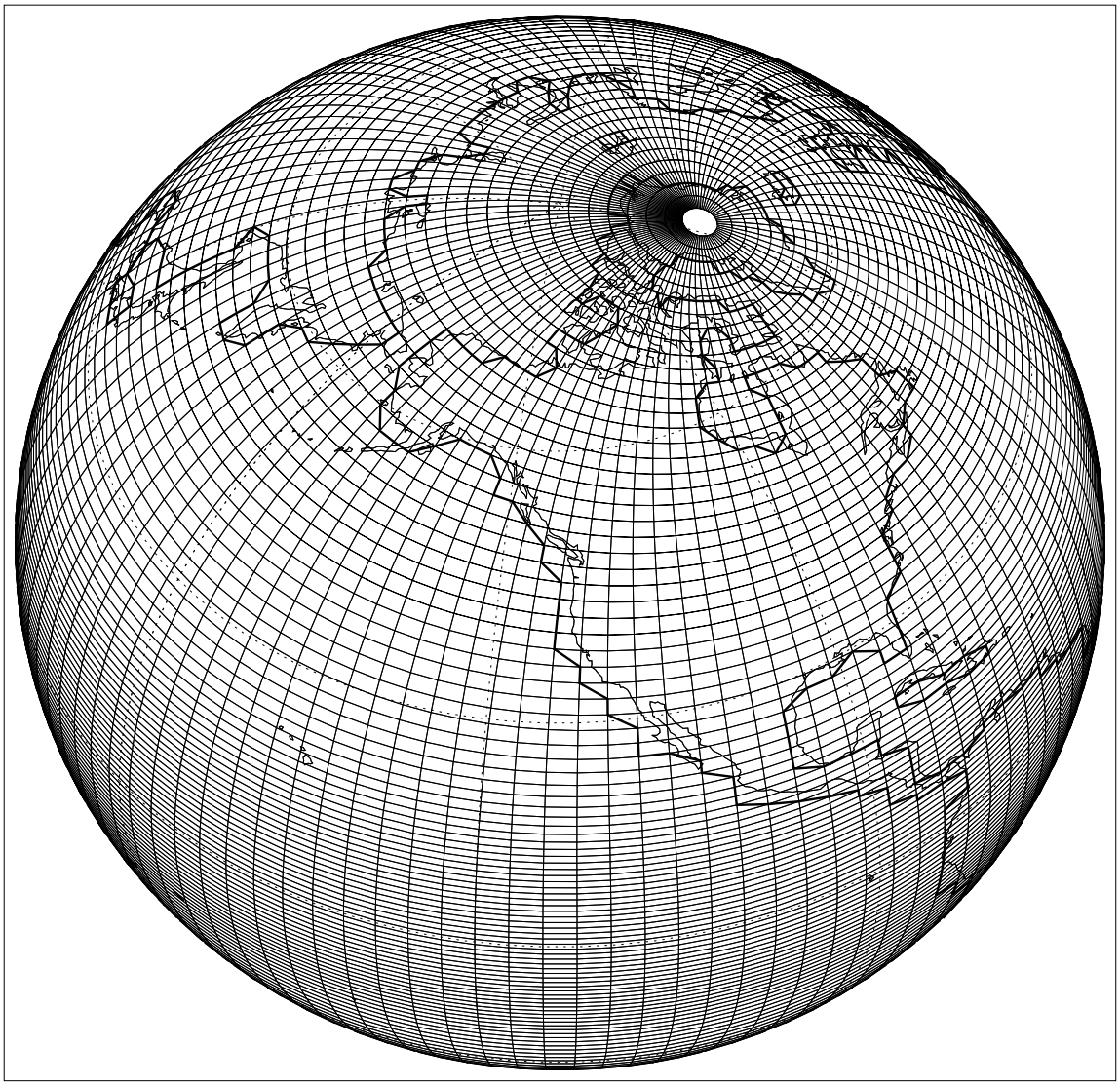

Figure 1: 3° global grid with the north pole singularity in Greenland.

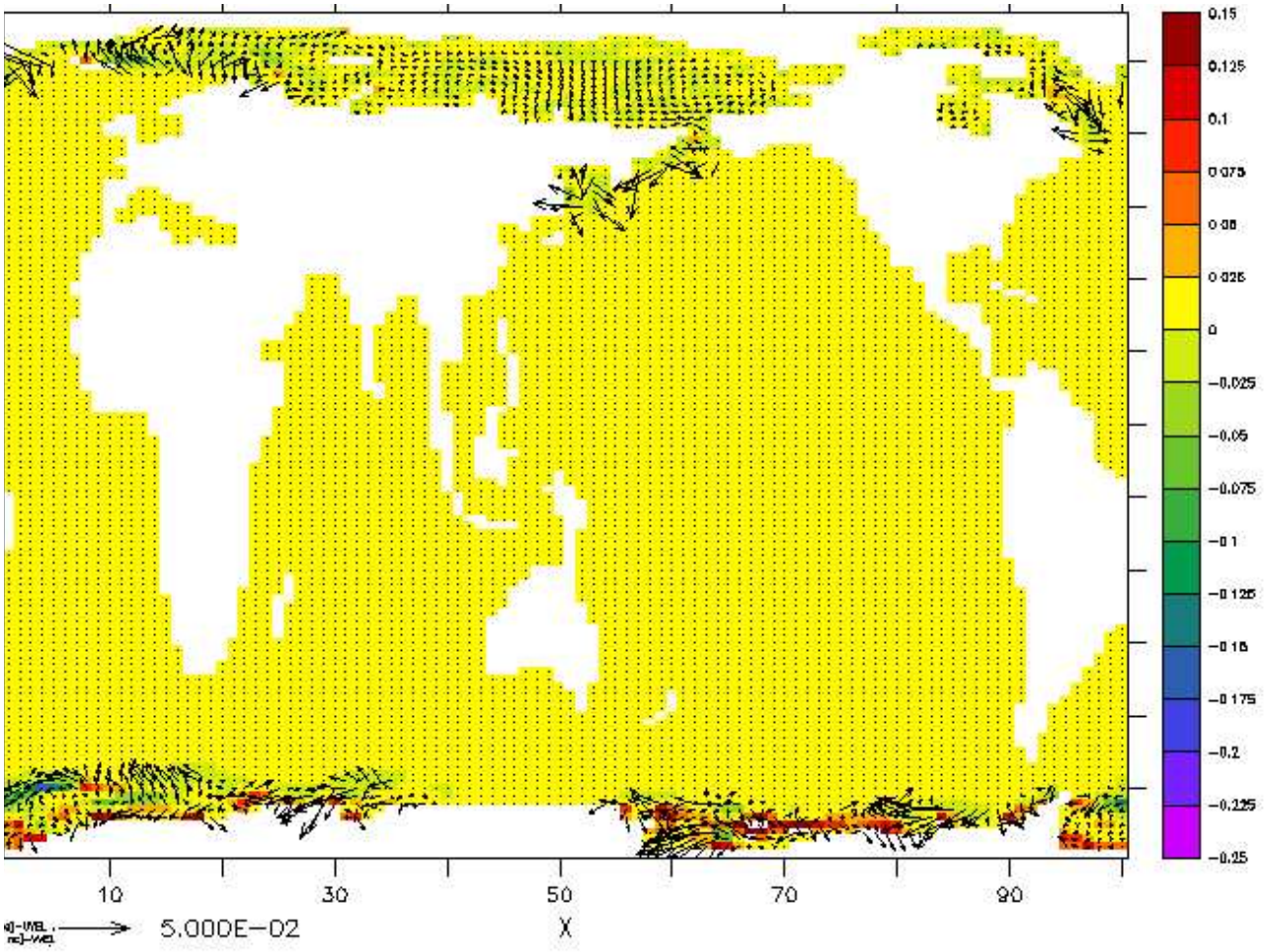

Figure 2: Difference in ice area fraction (color) and velocity difference vectors (test-control, m/s) for January of year 30, plotted in logical space.

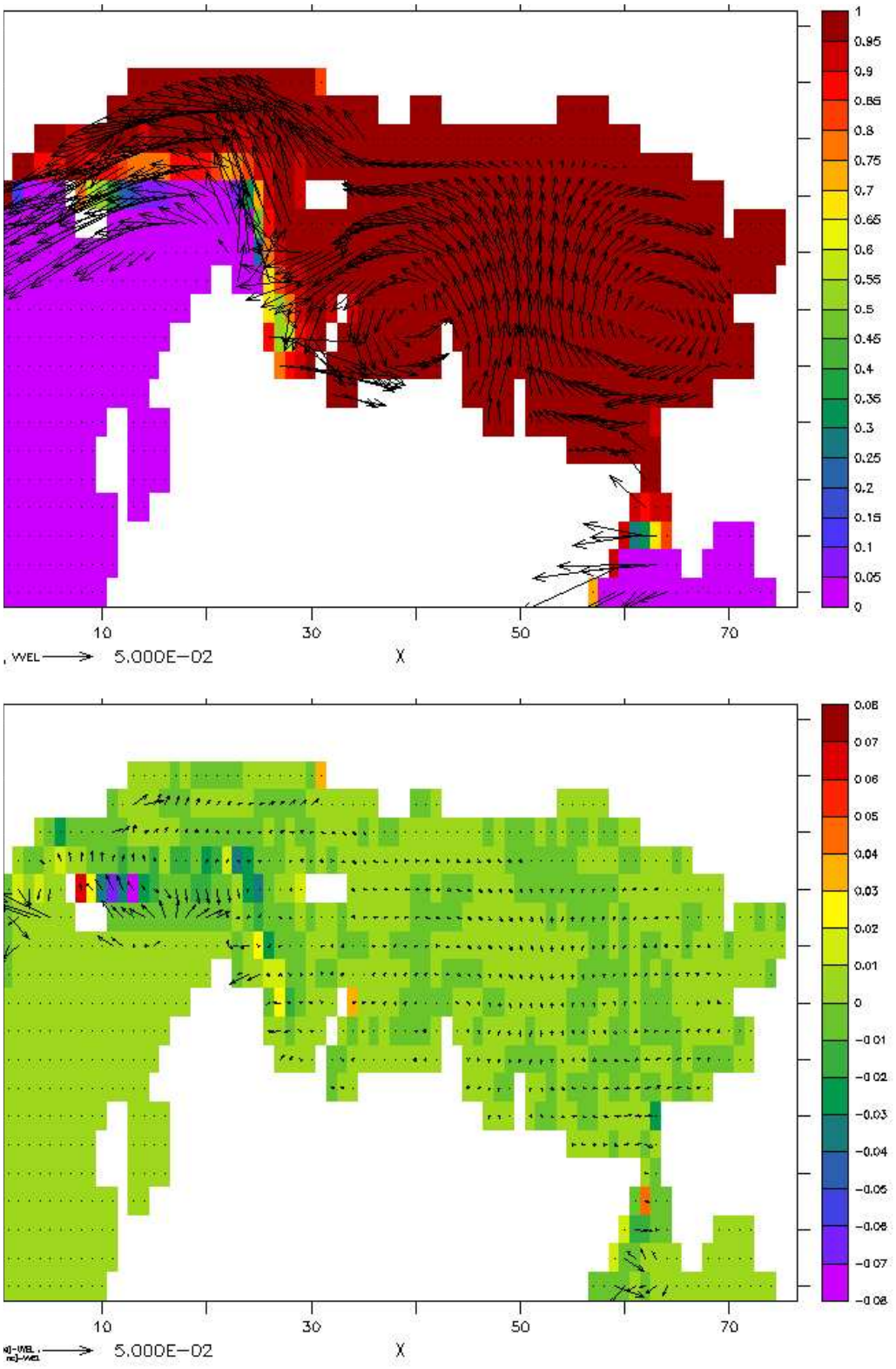

Figure 3: Arctic ice area fraction and velocity (m/s) for January, year 30. (a) control, (b) test-control.

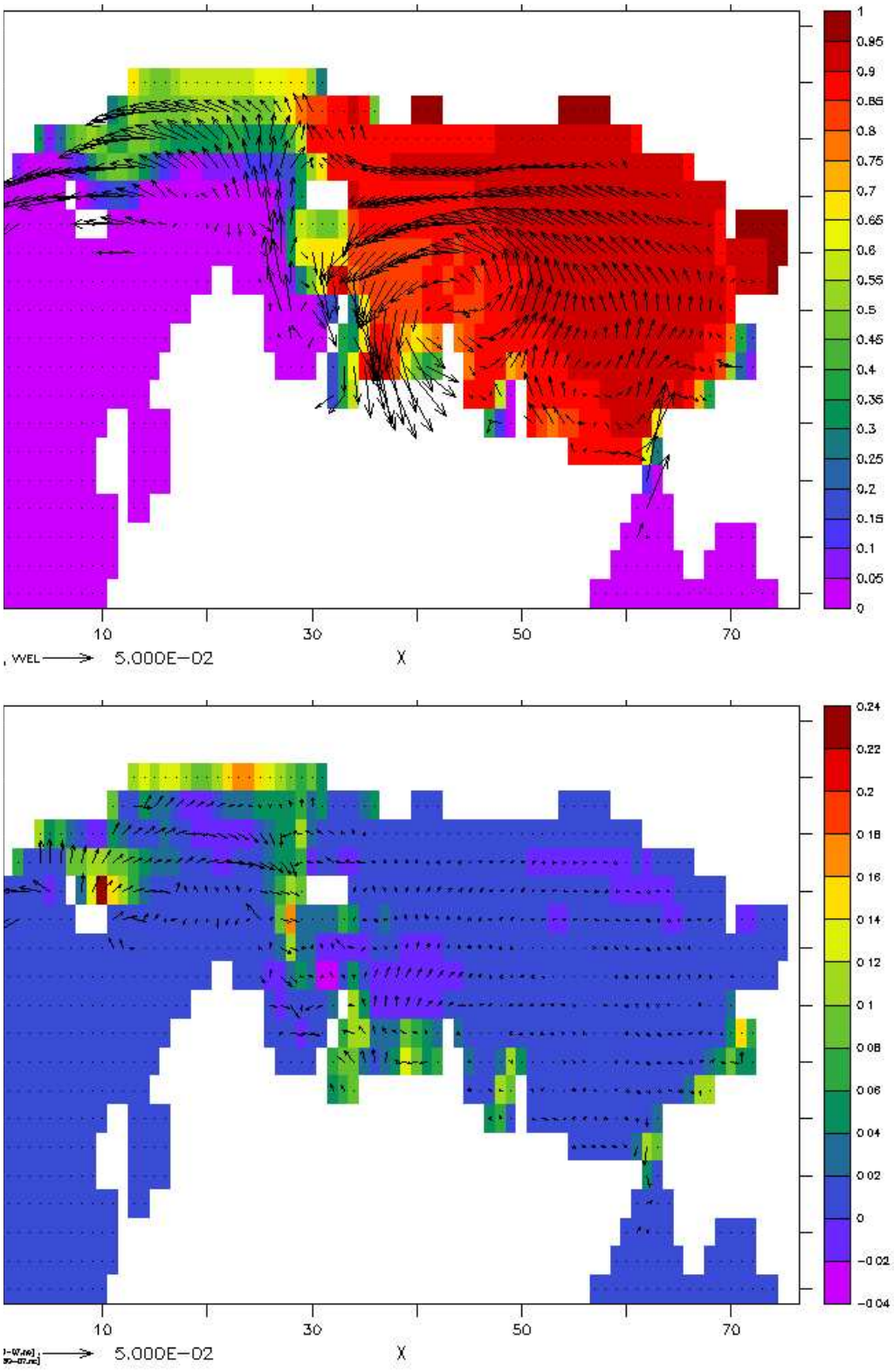

Figure 4: Arctic ice area fraction and velocity (m/s) for July, year 30. (a) control, (b) test-control.

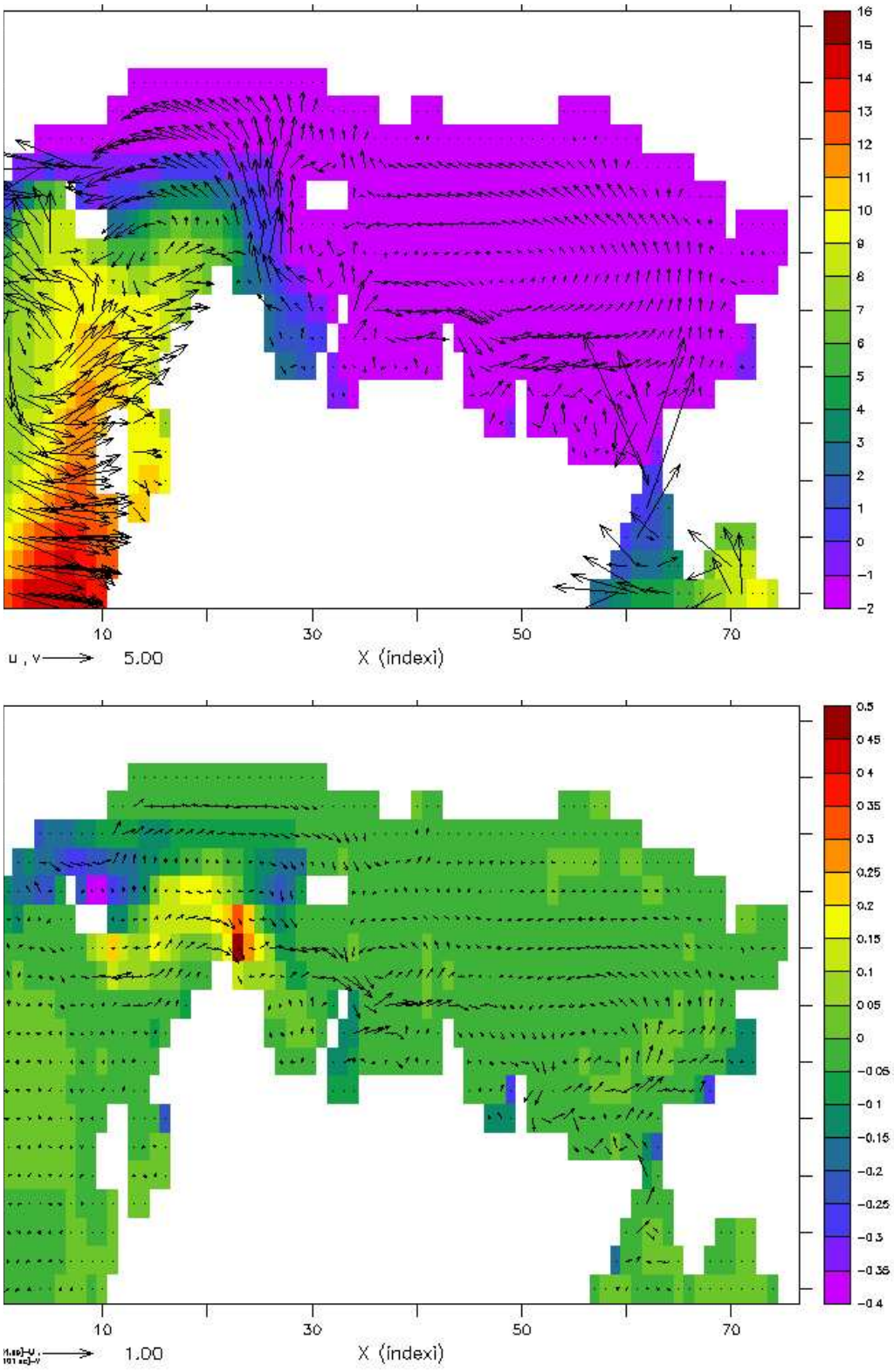

Figure 5: Mean annual Arctic SST (°C) and surface currents (cm/s) for year 30. (a) control, (b) test-control.